catalysts

MDPI

Article

Selective Oxidation of Glycerol Using 3% H_2O_2 Catalyzed by Supported Nano-Au Catalysts

Xiaoli Wang, Gongde Wu *, Tongfa Jin, Jie Xu and Shihao Song

Department of Environment and Technology, Nanjing Institute of Technology, Nanjing 211167, China; wangxiaoli212@njit.edu.cn (X.W.); jintongfa@njit.edu.cn (T.J.); jiexu@163.com (J.X.); shihaosongnjit@163.com (S.S.)

* Correspondence: wugongde@njit.edu.cn; Tel./Fax: +86-25-8611-8960

Received: 13 September 2018; Accepted: 25 October 2018; Published: 29 October 2018

Abstract: A series of transition metal oxides or mixed oxides supported nano-Au catalysts were prepared for the selective oxidation of glycerol to glyceric acid using 3% H_2O_2. It was found that the composition and structure of supports significantly influenced the catalytic performance of catalysts. The mesoporous trimetal mixed oxide (CuNiAlO) supported nano-Au catalysts were more active in comparison with the others. In the present catalytic system, the highest glycerol conversion was 90.5%, while the selectivity of glyceric acid could reach 72%. Moreover, the catalytic performance remained after 11 times of reaction.

Keywords: Au; mixed oxides; selective oxidation; glycerol; glyceric acid

1. Introduction

Environmental pollution and energy crisis are two major problems in the current world, so the synthesis of biodiesel from natural oils and fats has attracted much attention in recent years. By the end of 2015, the world's annual output of biodiesel has exceeded 30 million tons, at the same time, 1.54 million tons of by-product glycerol (GLY) was produced in the production process of biodiesel [1]. Thus, it has become an urgent problem how to utilize efficiently GLY. The common conversion pathways of GLY include selective oxidation, directional reduction, production of polymer, and esterification [1–6]. The selective oxidation of GLY could give many high value-added fine chemical products, such as glyceraldehyde, glyceric acid (GLYAC), and 1,3-dihydroxyacetone. Among them, GLYAC is an important substance in biochemical research, which can be used in the fields of muscle physiology, pharmaceutical, organic synthesis, etc. However, the present production methods of GLYAC are far from satisfactory to meet the requirements of the market, and the price of GLYAC is very high [2,6]. Therefore, it is of high scientific significance and practical value to study the selective oxidation of GLY to produce GLYAC in depth.

In recent years, many noble metal catalytic systems of ruthenium, molybdenum, tungsten, cobalt, chromium, manganese, gold, palladium, platinum, etc. were designed for the selective oxidation of GLY [3,4,6–18]. Although such catalysts were expensive, they showed irreplaceable high catalytic performance. Therefore, the design of effective noble metal catalysts was still eye-catching in current research. Compared to the other noble metal catalysts, gold catalysts could be used in the oxidation of alcohols under more mild conditions. Especially, the supported nano-Au particles could not only reduce the cost of catalyst preparation, but could also obtain highly active and reusable heterogeneous catalysts due to the introduction of support with high specific surface area [7–21]. Davis et al. [7] reported that supported Au/TiO_2 was active for the selective oxidation of GL. Sobczak et al. [8] found that AuCu-ZnO could effectively catalyze oxidation of GLY to produce GLYAC because of the electron transfer between metals due to the introduction of Cu. Órfão et al. [9] also used multi-walled carbon

nanotubes supported Au catalysts (Au/MWNTs) in the selective oxidation of GLY, and high catalytic activity was found accompanied by relatively low selectivity of GLYAC. However, in the reported catalytic system, the yield of GLYAC was less than 50%; moreover, homogeneous alkali NaOH was usually required to facilitate the reaction, which inevitably increased the cost of post-processing of products. Therefore, there is still an urgent need to design environmentally friendly and highly efficient supported Au catalysts for the selective oxidation of GLY to GLYAC. In our previous report, we had prepared a Cr_2O_3 supported nano-Au catalyst for this conversion under the condition of no alkaline additives; however, the catalytic performance was relatively low [9]. In the present investigation, nano-Au particles were further loaded on a series of mesoporous supports (transition metal oxides or mixed oxides) with different composition and structure. The catalytic performance of the obtained catalysts was investigated in the selective oxidation of GLY with 3% H_2O_2. The roles of composition and structure of support, the reaction conditions in the catalytic performance of catalysts were also discussed in detail.

2. Results and Discussion

2.1. Characterization of Catalysts

Considering the similarity of composition and structure in metal oxides or mixed oxides supported Au catalysts, the characterization of Au/Cr_2O_3, Au/CuO, and Au/CuNiAlO were selected as the representative to be illustrated here. The N_2 adsorption-desorption isotherms of Au/Cr_2O_3, Au/CuO and Au/CuNiAlO are typically shown in Figure 1. They all displayed type IV isotherms according to the IUPAC (International Union of Pure and Applied Chemistry), suggesting the presence of mesostructures. Simultaneously, the average pore sizes of Au/Cr_2O_3, Au/CuO, and Au/CuNiAlO were found to be 23.5, 20.4, and 15.2 nm, respectively. This mesoporous channels might be originated from the accumulation of catalyst particles. Textural properties of samples are listed in Table 1. Compared to the parent oxides, the Au supported catalysts exhibited decreased BET surface area due to the loading of Au.

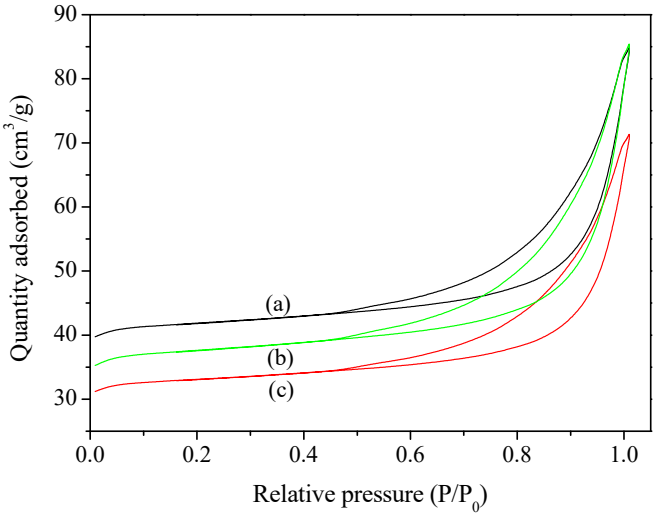

Figure 1. N_2 adsorption-desorption isotherm of simples; (**a**) Au/CuNiAlO, (**b**) Au/Cr_2O_3, and (**c**) Au/CuO.

The XRD patterns of three typical supported Au catalysts are illustrated in Figure 2. It was found that a new peak at about 38.18° related to elemental Au was detected in the spectra of Au/Cr_2O_3 and Au/CuNiAlO [10,22]. This indicated that the Au element might exist mainly in the form of 0 valent Au nanoparticles. However, such a characteristic peak at about 38.18°did not appear in the spectra of Au/CuO, probably because the characteristic peak assigned to Au nanoparticles was weak due to their

low loading, and was overlapped by the strong characteristic peaks of support CuO. In addition, in the XRD patterns of Au/CuNiAlO, the characteristic peak assigned to the pure metal oxides appeared, indicating the absence of alloys or intermetallic compound.

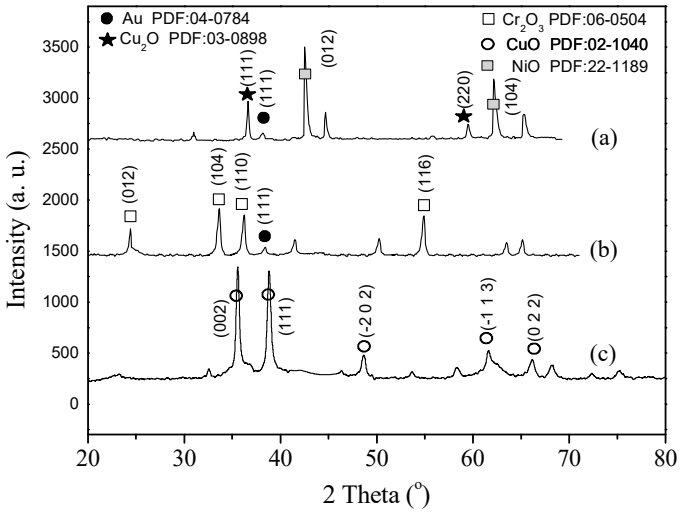

Figure 2. XRD patterns of samples; (**a**) Au/CuNiAlO, (**b**) Au/Cr_2O_3, and (**c**) Au/CuO.

Table 1. Textural properties and catalytic performance of different catalyst samples.

Entry	Catalysts	Au Loading (wt %)	Molar Ratio ($M_1/M_2/M_3$)	S_{BET} ($m^2\ g^{-1}$)	Au/S_{BET} [a] (mol m^{-2} × 10^{-7})	GLY Con. (%)	GLYAC Sel. (%)	H_2O_2 Efficiency (%)
1	Cr_2O_3	……	……	45	……	13.8	0	15.5
2	CuO	……	……	42	……	12.5	0	13.8
3	NiO	……	……	40	……	11.9	0	12.0
4	CoO	……	……	47	……	7.5	0	8.7
5	ZnO	……	……	45	……	4.0	0	5.1
6	Fe_2O_3	……	……	39	……	6.3	0	7.2
7	MCM-41	……	……	1020	……	0	0	0
8	SBA-15	……	……	785	……	0	0	0
9	CuNiAlO	……	Cu/Ni/Al = 0.85/0.85/1	220	……	38.5	27.3	41.5
10	FeNiAlO	……	Fe/Ni/Al = 0.86/0.87/1	223	……	22.1	12.2	24.6
11	CoNiAlO	……	Co/Ni/Al = 0.85/0.84/1	219	……	25.0	19.5	27.3
12	CrNiAlO	……	Cr/Ni/Al = 0.85/0.83/1	218	……	33.6	30.1	37.0
13	ZnNiAlO	……	Zn/Ni/Al = 0.85/0.86/1	221	……	23.0	16.9	25.9
14	Au/Cr_2O_3	0.95	……	37	13.0	81.5	67.0	83.0
15	Au/CuO	0.96	……	35	13.9	83.0	68.2	85.5
16	Au/NiO	0.92	……	35	13.3	65.7	58.5	67.2
17	Au/CoO	0.93	……	39	12.1	51.3	57.0	57.5
18	Au/ZnO	0.91	……	38	12.2	50.5	53.7	52.3
19	Au/Fe_2O_3	0.95	……	32	15.0	65.0	54.8	69.2
20	Au/MCM-41	0.98	……	976	0.5	33.2	77.6	37.5
21	Au/SBA-15	0.95	……	702	0.7	35.8	76.3	38.1
22	Au/CuNiAlO	0.93	Cu/Ni/Al = 0.85/0.86/1	206	2.3	90.5	72.0	89.5
23	Au/FeNiAlO	0.95	Fe/Ni/Al = 0.86/0.86/1	203	2.4	79.7	65.4	80.2
24	Au/CoNiAlO	0.92	Co/Ni/Al = 0.85/0.85/1	205	2.3	73.0	63.1	76.4
25	Au/CrNiAlO	0.90	Cr/Ni/Al = 0.85/0.84/1	203	2.2	89.5	70.8	87.3
26	Au/ZnNiAlO	0.94	Zn/Ni/Al = 0.86/0.85/1	202	2.4	60.5	60.0	67.0

[a] Molar mass of Au per surface area; Reaction conditions: GLY 10 mmol, 3% H_2O_2 25 mL, Catalyst 0.2 g, 60 °C, 4 h.

The XPS characterization was further employed to understand the chemical states of Au species in catalysts (see Figure 3), and no significant difference was found. The Au4f binding energy of the three typical samples all appeared at 83.8 ev and 87.4 ev, indicating that the Au species were all elementary substance in catalysts [10,23]. The TEM images also showed that the sizes of Au particles in catalyst was about 2~6 nm (see Figure 4), further conforming the presence of Au nanoparticles. In addition, typically we also calculated the crystallite size of Au particles in Au/CuNiAlO of 4.5 nm

and Au/Cr_2O_3 of 2.7 nm by Scherrer formula from the position of $2\theta = 38.18°$ peak in Figure 2, which is comparable with the result of TEM. Thus, the difference in the catalytic performance of the three catalysts might be originated from their different support.

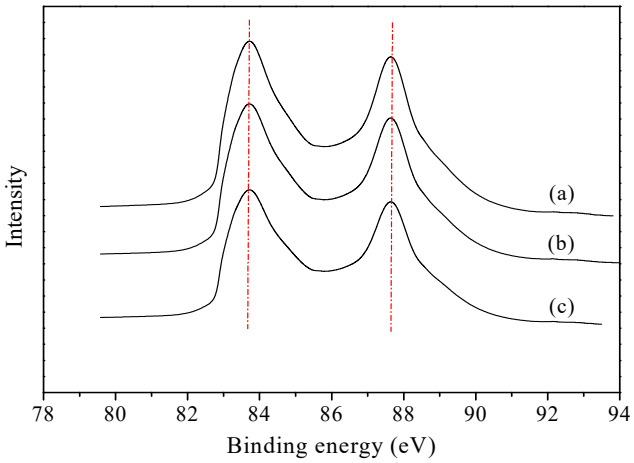

Figure 3. XPS of Au4f in samples; (**a**) Au/CuNiAlO, (**b**) Au/Cr_2O_3, and (**c**) Au/CuO.

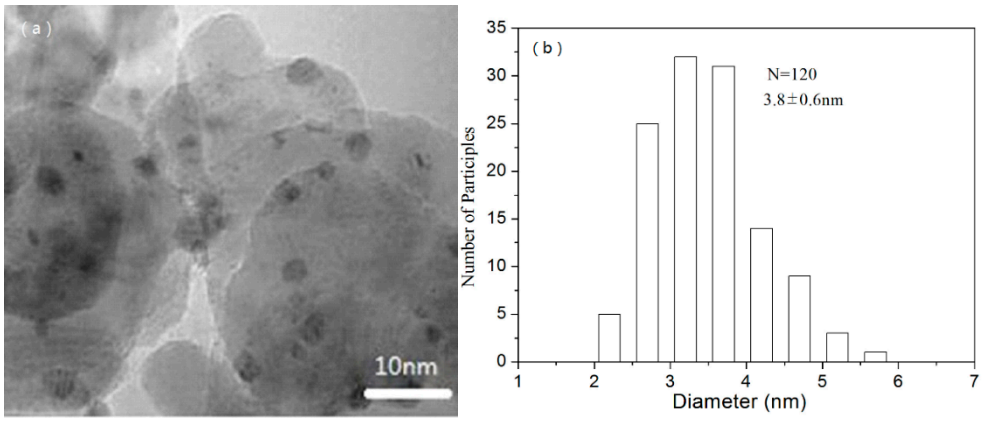

Figure 4. TEM image (**a**) and particle size distribution (**b**) of Au/CuNiAlO (×90,000; 30.0 kV).

2.2. Catalytic Performance

The obtained catalysts were used in the selective oxidation of GLY to GLYAC by 3% H_2O_2. The results in Table 1 showed that only slight catalytic activity was detected over six single metal oxide catalysts, while no object product of GLYAC was detected, and the main product was the low added value formic acid. When the trimetal mixed oxides was used as catalysts, both the GLY conversion and GLYAC selectivity increased significantly. This might be because the coexistence of three metal elements increased the disorder degree of catalysts, and led to more co-catalytic active sites being exposed to the oxidation reaction. Among them, CuNiAlO and CrNiAlO exhibited higher catalytic performance, though all the trimetal mixed oxides showed the similar surface area and molar ratio of metal element. This also indicated that the surface area and molar ratio of metal element did not significantly affect the reaction; it was the different element type of catalysts that could afford their different catalytic performance. It seems that Cu, Ni, and Cr, in comparison with the other transition metal elements, was more active for the GLY oxidation, which might be related to their relatively high H_2O_2 efficiency; similar phenomena was also found in our previous report [23,24]. Furthermore, upon introducing the Au nanoparticles to the surface of the above oxides, the supported nano-Au catalysts exhibited remarkably enhanced catalytic performance and H_2O_2 efficiency than their corresponding oxide parents. This suggested that Au nanoparticles were also key active sites in the present selective oxidation of GLY. In order to investigate the catalytic activity of Au nanoparticles,

they were further loaded on two typical mesoporous media of MCM-41 and SBA-15 with high specific surface but no active transition metal elements. It was found that the obtained supported Au catalysts exhibited lower catalytic performance than the other transition metal oxides supported catalysts. This revealed that there might be some interaction between transition metal oxide carriers and Au nanoparticles, which determined the catalytic performance of supported Au catalysts together. In the present investigation, the Au/CuNiAlO exhibited the GLY conversion of 90.5% and the GLYAC selectivity of 72%, though all the trimetal mixed oxides supported Au catalysts showed the similar surface area and local Au concentration.

The effect of reaction conditions on the catalytic performance of Au/CuNiAlO was also investigated. The results revealed that the dosage of catalyst and oxidant, the reaction temperature and time all remarkably influenced the catalytic performance of catalyst (see Figure 5). When the reaction was run at 60 °C for 4 h with 10 mmol GLY, 25 mL 3% H_2O_2 and 0.2 g catalyst, the optimal catalytic results could be obtained.

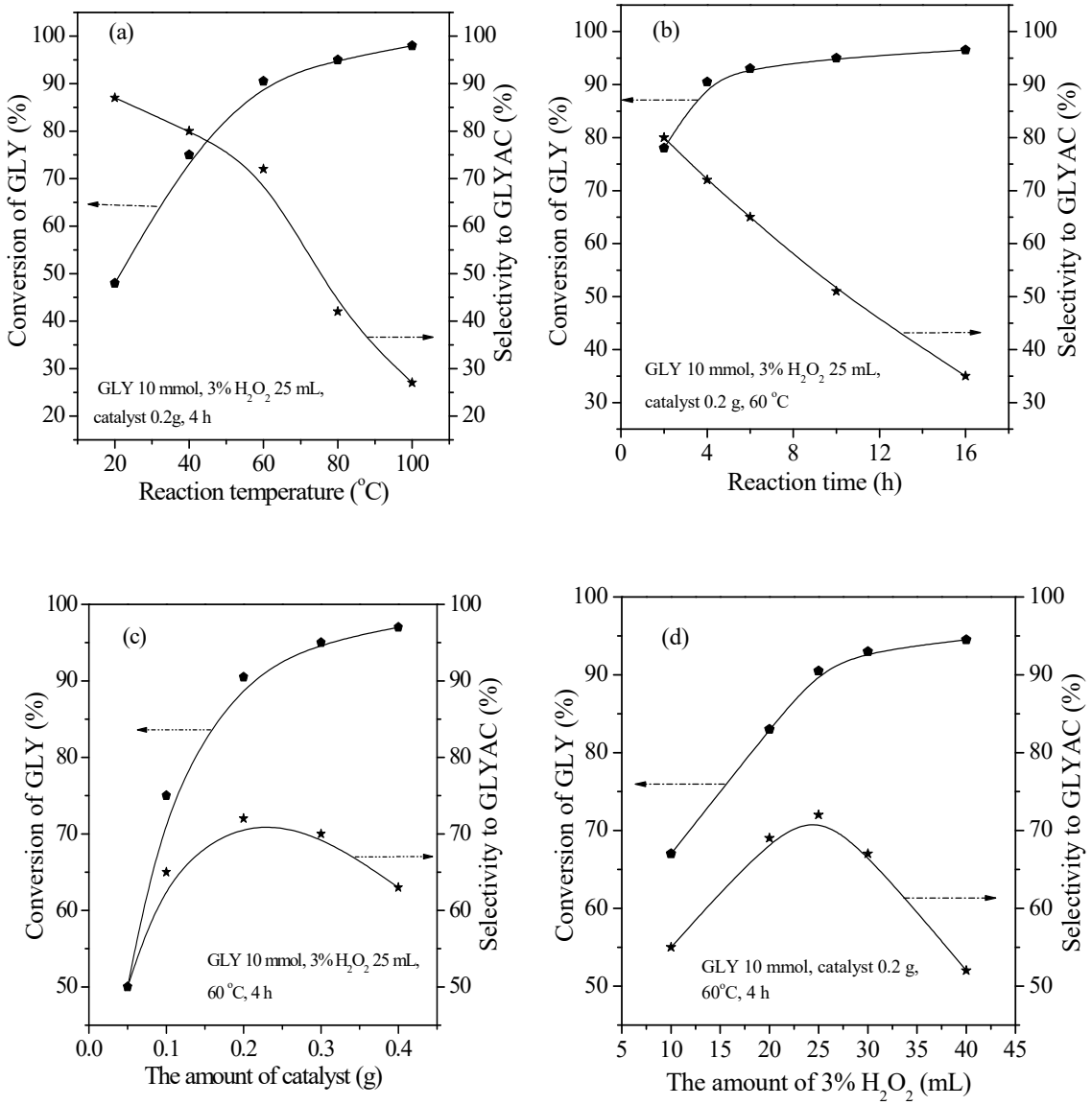

Figure 5. Effect of reaction conditions on the catalytic performance of catalyst, (**a**) Reaction temperature, (**b**) Reaction time, (**c**) the amount of catalyst, (**d**) the amount of 3% H_2O_2.

The recyclability of Au/CuNiAlO was also studied in the selective oxidation of GLY to GLYAC. After the first reaction, the catalyst was filtered out from the reaction mixture, washed with deionized water to remove the physisorbed reactant or product molecules, dried and then reused in another 10 catalytic runs. The results in Figure 6 illustrated that the catalyst was still effective for at least 11 times, indicating the excellent stability of this catalyst in the present reaction condition.

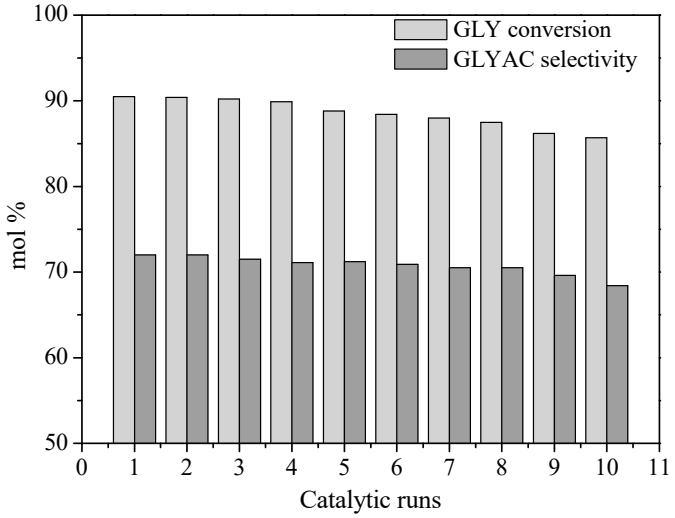

Figure 6. Reusability of Au/CuNiAlO in the selective oxidation of GLY. Reaction conditions: GLY 10 mmol, 3% H_2O_2 25 mL, Catalyst 0.2 g, 60 °C, 4 h.

To further investigate the stability of Au/CuNiAlO, the leaching test was studied. Figure 7 gives the time-conversion plot of the twin reactions with and without catalyst. The results revealed that the reaction after filtering catalyst performed slowly, and only slight increase with the increased reaction time in the GLY conversion was found due to the nonselective catalytic oxidation. This further confirmed that the catalyst had good stability under the current reaction conditions.

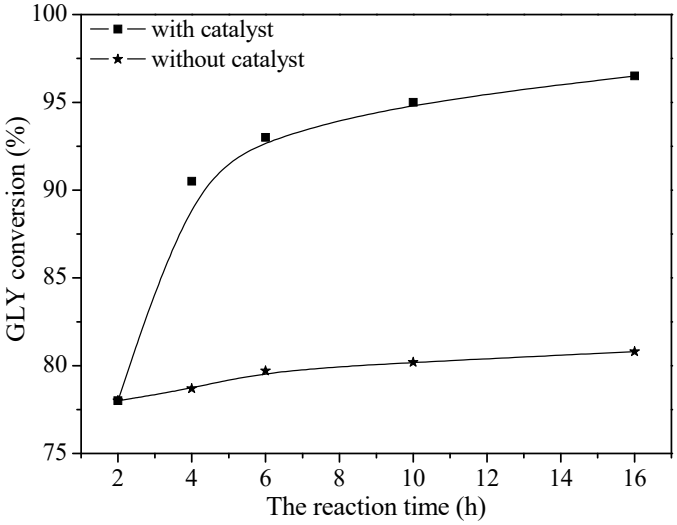

Figure 7. Effect of leaching of Au/CuNiAlO on the GLY oxidation Reaction conditions: GLY 10 mmol, 3% H_2O_2 25 mL, Catalyst 0.2 g, 60 °C.

2.3. Reaction Process

The continuous interests in the mechanism of glycerol oxidation pushed us to further investigate the reaction process in the present catalytic system. Au/CuNiAlO was selected as the representative catalyst for this investigation. The selectivity of the main and by-products at different reaction

temperatures to the glycerol conversion rate was plotted in Figure 8. It was found that the selectivity of the object product GLYAC decreased, while the selectivity of Glycolic acid, Tartronic acid and Formic acid increased with the enhanced GLY conversion. This indicated that Glycolic acid, Tartronic acid and Formic acid might be the further oxidation or decomposition products of the produced GLYAC. Simultaneously, 1,3-dihydroxyacetone was not detected here, indicating that the present reaction environment is more conducive to GLY oxidation to glyceraldehyde. Considering that the main product was GLYAC, the oxidation of glyceraldehyde to GLYAC should be more rapidly than the oxidation of GLY to glyceraldehyde. Thus, we speculated that the GLY oxidation in the present catalytic system might proceed the following reaction process. Namely the substrate of GLY firstly underwent oxidative dehydrogenation to produce glyceraldehyde, and then the obtained aldehyde was further oxidized to GLYAC. Furthermore, GLYAC also underwent the side reaction of overoxidation and/or decarboxylation to give Glycolic acid, Tartronic acid and Formic acid (see Scheme 1).

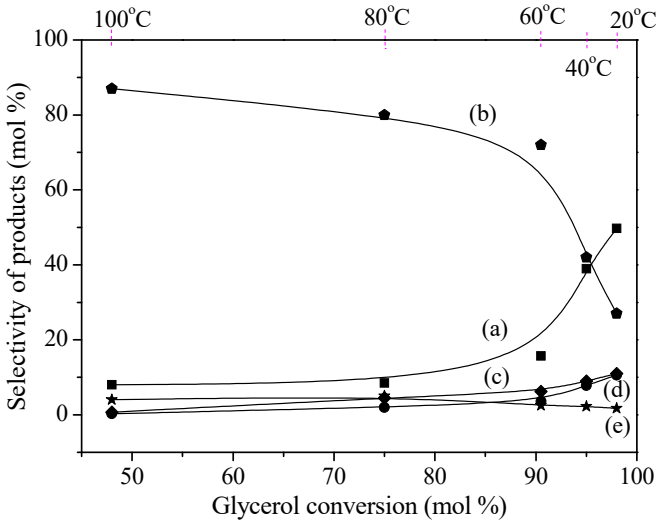

Figure 8. The correlation between the glycerol conversion and the selectivity of products at different reaction temperature. (**a**) GLYAC, (**b**) Formic acid, (**c**) Glycolic acid, (**d**) Tartronic acid, (**e**) Glyceraldehyde. Reaction conditions: GLY 10 mmol, 3% H_2O_2 25 mL, Catalyst 0.2 g, 4 h.

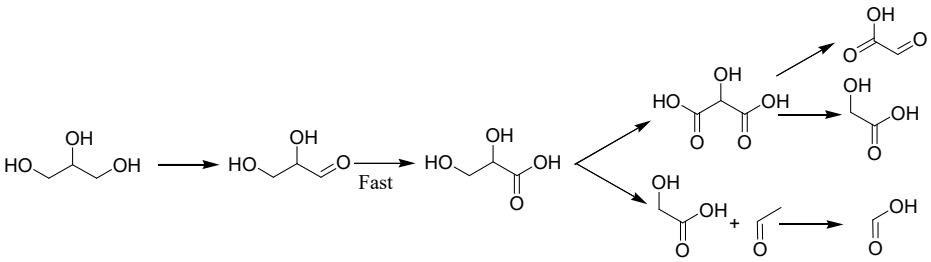

Scheme 1. Possible reaction pathway for glycerol oxidation.

3. Experimental Section

3.1. Catalyst Preparation

3.1.1. Preparation of Single Metal Oxides

Typically, a 1 mol/L $Na_2CO_3 \cdot 10H_2O$ solution was added dropwise to a 45 mL aqueous solution contained 0.045 mol of metal nitrate $M(NO_3)_x \cdot nH_2O$ (M = Cr^{3+}, Fe^{3+}, Co^{2+}, Ni^{2+}, Cu^{2+}, Zn^{2+}) with vigorous stiring at 400 rpm and 25 °C. In the process of dropping, the pH value of mixture was controlled at about 10 by adding appropriate amount of NH_4OH (35% aqueous ammonia solution). The resulting mixture was further aged for 12 h at room temperature, and then was filtrated and

washed with deionized water. The precipitate was dried at 60 °C for 24 h, and then was calcined at 350 °C for 4 h.

3.1.2. Preparation of Polymetallic Mixed Oxides

Polymetallic mixed oxides were prepared by calcinating the polymetallic hydrotalcites as described in our previous report [23]. Typically, a 100 mL 1 mol/L nitrite solution contained equivalent three kinds of metal cations and a 100 mL 1 mol/L Na_2CO_3 aqueous solution were simultaneously added dropwise to 100 mL deionized water with stirring at 400 rpm and room temperature. During addition, the pH value of mixed solution was maintained at 10.0 ± 0.5 by adding appropriate amounts of NaOH. The resulting mixture was hydrothermally treated at 100 °C for 24 h in an autoclave with polytetrafluoroethylene lining. The precipitate was collected after being filtered, washed with deionized water and dried at 100 °C for 12 h. Then, the solid sample was further calcined under a flowing stream of pure nitrogen in an oven at 450 °C for 8 h. In this way, a series of trimetal mixed oxides were prepared and denoted as $M_1M_2M_3O$ (M_1, M_2 and M_3 was three different transition metals; such as Cr^{3+}, Fe^{3+}, Co^{2+}, Ni^{2+}, Cu^{2+} and Zn^{2+})

3.1.3. Preparation of Au Loaded Oxides

1 g metal oxide prepared above, 2 mL 0.5 mol/L chloroauric acid solution and 2.44 g urea were added to a three-necked bottle with 50 mL deionized water. The mixture was stirred (400 rpm) for 6 h at 80 °C and another 12 h at room temperature, and then was filtered, washed with deionized water. The solid residue was dried under vacuum at 60 °C for 24 h, and then was calcined at 200 °C for 4 h.

3.2. Characterization

The gold contents in the samples were determined by inductively coupled plasma emission spectroscopy (PerkinElmer ICP OPTIMA-3000, Thermo Electron, Waltham, MA, USA). The BET specific surface area was measured and calculated by N_2 adsorption-desorption method on an ASAP 2000 automatic physical adsorption apparatus (Micromeritics, Norcross, GA, USA) using static adsorption procedures. Before testing, the samples were degassed at 1×10^{-4} Pa and 80 °C for 10 h. Surface area (S_{BET}) was calculated by the BET method, and the average pore diameter was calculated by the BJH method from the desorption isotherm. Powder X-ray diffraction experiments (XRD) were performed at 50 kv and 30 mA on a Rigaku Miniflex diffractometer (Rigaku Corporation, Tokyo, Japan), which was equipped with Cu Kα radiation. The wide-angel patterns were recorded in a range of 5–70° at a scan rate of 0.2°/min. Transmission electron microscope studies (TEM) were carried out by a JEOL JEM 2100 microscope (Hitachi, Akishima, Japan). The particle size distribution of Au was calculated by counting approximately 120 particles in TEM images. The X-ray photoelectron spectroscopy (XPS) of samples was got by a PHI 5000 VersaProbe X-ray photoelectron spectrometer (ULVAC-PHI Co. Kanagawa, Japan) with monochromatic Al X-rays (1486.6 ev) at 15 mA and 15 kV.

3.3. Catalytic Test

Typically, 25 mL 0.4 mol/L GLY aqueous solution and a certain amount of catalyst (80 meshes; 0.05, 0.1, 0.2, 0.3 or 0.4 g) were added to a three neck flask (100 mL), and then was being magnetic stirred at 600 rpm and room temperature for 10 min. The mixture was heated to the desired temperature (20, 40, 60, 80 or 100 °C) within 5 min; a required amount of 3% H_2O_2 (10, 20, 25, 30 or 40 mL) was further dripped. After the reaction performed for several hours (2, 4, 6, 10 or 16 h) under stirring (600 r/min), the catalyst was filtered out. The residue was sent to HPLC (High Performance Liquid Chromatography) with an Aminex HPX-87H column (Bio-Rad, Philadelphia, PA, USA), and 0.01 mol/L H_2SO_4 was selected as eluent flowing at 0.5 mL/min. H_2O_2 consumption was determined after the reactions by iodometric titration.

4. Conclusions

The supported nano-Au catalysts were effective catalysts in the selective oxidation of GLY to GLYAC. Among them, the mesoporous mixed oxides supported nano-Au catalysts exhibited high catalytic performance because of the interaction between the active nano-Au particles and the support. Compared to the single oxides supported catalysts, in the mixed oxides supported catalysts, the presence of multiple metal elements in support might had led to a high system disorder, and thus more co-catalytic active sites on support surface were exposed to the oxidation reaction, which could afford their much higher catalytic performance. Under the best reaction conditions, the highest GLY conversion was 90.5%, and the selectivity of GLYAC was 72%. Moreover, this catalyst also exhibited high catalytic reusability, which could be reused 11 times.

Author Contributions: G.W. and X.W. designed the experiments; X.W. analyzed the data and wrote the paper; T.J., J.X. and S.S. performed the experiments.

Funding: This research received no external funding.

Acknowledgments: The authors acknowledge the financial supports from National Natural Science Foundation of China 21203093, Natural Science Foundation of Jiangsu Province BK20141388 and BK20161481, Research Joint Research Project of Jiangsu Province BY2016008-03, Key Research and Development Program of Jiangsu Province BE2018718, and College Students Practice Innovation Training Program of Nanjing Institute of Technology TP20161201 and TZ20170023.

Conflicts of Interest: No conflict of interest was declared here.

References

1. Cespi, X.D.; Passarini, F.; Mastragostino, G.; Vassura, I.; Larocca, S.; Iaconi, A.; Chieregato, A.; Duboise, J.L.; Cavani, F. Glycerol as feedstock in the synthesis of chemicals: A life cycle analysis for acrolein production. *Green Chem.* **2015**, *17*, 343–355. [CrossRef]
2. Xiang, Y.Z.; Davis, R.J. Glycerol-intercalated Mg-Al hydrotalcite as a potential solid base catalyst for transesterification. *Clay Clay Miner.* **2010**, *58*, 475–485.
3. Zhou, C.H.; Beltramini, J.N.; Fan, Y.X.; Lu, G.Q. Chemoselective catalytic conversion of glycerol as a biorenewable source to valuable commodity chemicals. *Chem. Soc. Rev.* **2008**, *37*, 527–549. [CrossRef] [PubMed]
4. Zhang, Ch.; Wang, T.; Ding, Y.J. One-step synthesis of pyruvic acid from glycerol oxidation over Pb promoted Pt/activated carbon catalysts. *Chin. J. Catal.* **2017**, *38*, 928–938. [CrossRef]
5. Zhang, Ch.; Wang, T.; Liu, X.; Ding, Y.J. Cu-promoted Pt/activated carbon catalyst for glycerol oxidation to lactic acid. *J. Mol. Catal. A Chem.* **2016**, *44*, 91–97. [CrossRef]
6. Yu, K.O.; Kim, S.W.; Han, S.O. Reduction of glycerol production to improve ethanol yield in an engineered saccharomyces cerevisiae using glycerol as substrate. *J. Biotechnol.* **2010**, *150*, 209–214. [CrossRef] [PubMed]
7. Zope, B.N.; Hibbitts, D.D.; Neurock, M.; Davis, R.J. Reactivity of the gold/water interface during selective oxidation catalysis. *Science* **2010**, *330*, 74–77. [CrossRef] [PubMed]
8. Kaskow, I.; Decyk, P.; Sobczak, I. The effect of copper and silver on the properties of Au-ZnO catalyst and its activity in glycerol oxidation. *Appl. Surf. Sci.* **2018**, *444*, 197–207. [CrossRef]
9. Rodrigues, E.G.; Carabineiro, S.A.C.; Delgado, J.J.; Chen, X.; Pereira, M.F.R.; Órfão, J.J.M. Gold supported on carbon nanotubes for the selective oxidation of glycerol. *J. Catal.* **2012**, *285*, 83–91. [CrossRef]
10. Wang, X.L.; Wu, G.D.; Liu, X.F.; Zhang, F.; Xue, Y.B.; Tang, X.; Jin, T.F. Selective Oxidation of Glycerol to Glyceric Acid Catalyzed by Supported Nanosized Au/Cr_2O_3. *J. Mol. Catal. (China)* **2017**, *31*, 334–340.
11. Feng, J.J.; Chem, S.S.; Chen, X.L.; Zhang, X.F.; Wang, A.J. On-pot fabrication of reduced grapheme oxide supported dendritic core-shell gold @ gold-palladium nanoflowers for glycerol oxidation. *J. Colloid Interface Sci.* **2018**, *509*, 73–81. [CrossRef] [PubMed]
12. Liu, M.T.; Chen, L.X.; Li, D.N.; Wang, A.J.; Zhang, Q.L.; Feng, J.J. On-pot controlled synthesis of AuPd@Pd core-shell nanocrystals with enhanced electrocatalytic performances for formic acid oxidation and glycerol oxidation. *J. Colloid Interface Sci.* **2017**, *508*, 551–558. [CrossRef] [PubMed]

13. Kapkowski, M.; Bartczak, P.; Korzec, M.; Sitko, R.; Szade, J.; Balin, K.; Lelątko, J.; Polanski, J. SiO_2-, Cu-, and Ni-supported Au nanoparticles for selective glycerol oxidation in the liquid phase. *J. Catal.* **2014**, *319*, 110–118. [CrossRef]
14. Sharma, A.S.; Kaur, H.; Shah, D. Selective oxidation of alcohols by supported gold nanoparticles: Recent advances. *RSC Adv.* **2016**, *6*, 28688–28727. [CrossRef]
15. Prati, L.; Villa, A.; Chan-Thaw, C.E.; Arrigo, R.; Wang, D.; Su, D.S. Gold catalyzed liquid phase oxidation of alcohol: The issue of selectivity. *Faraday Discuss.* **2011**, *152*, 353–365. [CrossRef] [PubMed]
16. Rodrigues, E.G.; Pereira, F.R.; Chen, X.W.; Delgado, J.J.; Orfao, J.J.M. Selective oxidation of glycerol over platinm-based catalysts supported on carbon nanotubes. *Ind. Eng. Chem. Res.* **2013**, *52*, 17390–17398. [CrossRef]
17. Oliveira, L.C.A.; Portilho, M.F.; Silva, A.C.; Taroco, H.A.; Souza, P.P. Modified niobia as a bifunctional catalyst for simultaneous dehydration and oxidation of glycerol. *Appl. Catal. B Envioron.* **2012**, *117*, 29–35. [CrossRef]
18. Wang, F.F.; Shao, S.; Liu, C.L.; Xu, C.L.; Yang, R.Z.; Dong, W.S. Selective oxidation of glycerol over Pt supported on mesoporous carbon nitride in base-free aqueous solution. *Chem. Eng. J.* **2015**, *264*, 336–343. [CrossRef]
19. Zhang, M.Y.; Nie, R.F.; Wang, L.; Shi, J.J.; Du, W.C.; Hou, Z.Y. Selective oxidation of glycerol over carbon nanofibers supported Pt catalysts in a base-free aqueous solution. *Catal. Commun.* **2015**, *59*, 5–9. [CrossRef]
20. Zhao, G.F.; Yang, F.; Chen, Z.J.; Liu, Q.F.; Ji, Y.G.; Zhang, Y.; Niu, Z.Q.; Mao, J.J.; Bao, X.H.; Hu, P.J.; Li, Y.D. Metal/oxide interfacial effects on the selective oxidation of primary alcohols. *Nat. Commun.* **2017**, *8*, 14039. [CrossRef] [PubMed]
21. Tsuji, A.; Nishimura, S.; Takagaki, A.; Ebitani, K. Selective oxidation of glycerol by using a hydrotalcite-supported platinum catalyst under atmospheric oxygen pressure in water. *Chem. Sus. Chem.* **2011**, *4*, 542–548. [CrossRef] [PubMed]
22. Fujita, T.; Horikawa, M.; Takei, T.; Murayama, T.; Haruta, M. Correlation between catalytic activity of supported gold catalysts for carbon monoxide oxidation and metal-oxygen binding energy of the support metal oxides. *Chin. J. Catal.* **2016**, *37*, 1651–1655. [CrossRef]
23. Wu, G.D.; Wang, X.L.; Huang, Y.; Liu, X.F.; Zhang, F.; Ding, K.Q.; Yang, X.L. Selective oxidation of glycerol with O_2 catalyzed by low-cost CuNiAl hydrotalcites. *J. Mol. Catal. A Chem.* **2013**, *379*, 185–191. [CrossRef]
24. Wang, X.L.; Wu, G.D.; Wang, F.; Ding, K.Q.; Zhang, F.; Liu, X.F.; Xue, Y.B. Base-free selective oxidation of glycerol with 3% H_2O_2 catalyzed by sulphonato-salen-chromium(III) intercalated LDH. *Catal. Commun.* **2012**, *28*, 73–76. [CrossRef]